

# Development and Validation of a Novel Time-Resolved Laser-Induced Fluorescence Technique

IEPC-2013-356

*Presented at the 33rd International Electric Propulsion Conference,  
The George Washington University • Washington, D.C. • USA  
October 6 – 10, 2013*

Christopher J. Durot<sup>1</sup>, Alec D. Gallimore<sup>2</sup> and Timothy B. Smith<sup>3</sup>  
*University of Michigan, Ann Arbor, MI, 48105, USA*

**Abstract:** We present a novel technique to measure time-resolved laser-induced fluorescence (TRLIF) signals in plasma sources that have a relatively constant Fourier spectrum of oscillations in steady-state operation, but are not necessarily periodically pulsed or repeatable; e.g. Hall thrusters. The technique uses laser modulation on the order of MHz and recovers signal via a combination of band-pass filtering, phase-sensitive detection, and averaging over estimated transfer functions calculated for many different cycles of the oscillation. Periodic discharge current oscillations were imposed on a hollow cathode and the resulting oscillations in the LIF profile are observed. Measurements were validated by comparison with independent measurements of the average velocity distribution from a lock-in amplifier and by comparison with an independent time-resolved analysis technique. This new technique has a niche in measurements where the analog photomultiplier signal has a strong background signal with a nonwhite spectral density and the cycles of the oscillation are not sufficiently repeatable to allow for reliable triggering or a meaningful average waveform in the time domain. Hall thruster oscillations are one example of such conditions, and this technique will be used to interrogate unperturbed Hall thruster breathing and rotating spoke modes in future work.

## I. Introduction

A novel method of measuring a time-resolved laser-induced fluorescence (TRLIF) signal is described and validated in this paper. By time-resolved, we mean making LIF measurements in timescales commensurate with those of significant plasma property changes for a "steady" (i.e. not pulsed) plasma source with oscillations. This method has been developed for plasma sources with oscillations that have an approximately stationary spectrum, but do not have periodically repeatable oscillations that can be easily used to trigger averaging. Specifically, this method is intended to interrogate changes in the ion velocity distribution during Hall thruster breathing and spoke modes, which tend to exhibit approximately stationary Fourier spectra during stable thruster operation.

More precisely, we use a transfer function averaging technique that requires a time-invariant linear system, which implies that there is a constant transfer function describing the relationship between the spectra of output (LIF signal) and input (discharge current). This technique was first developed by for high-speed Langmuir probe measurements, and the success of that work justifies the applicability of the technique to Hall thruster oscillations<sup>1-3</sup>. As a test bed for the purposes of TRLIF validation, we impose a fixed-frequency oscillation on the discharge current between a hollow cathode and an anode and observe the resulting oscillations in LIF signal. The requirement of a time-invariant linear system may appear to be strict. On the contrary, this requirement is more loose than the implicit

---

<sup>1</sup> Ph.D. Candidate, Applied Physics, durot@umich.edu.

<sup>2</sup> Arthur F. Thurnau Professor, Aerospace Engineering, rasta@umich.edu.

<sup>3</sup> Lecturer, Aerospace Engineering, timsmith@umich.edu.

assumption of a triggered average in the time domain that there exists a repeatable process that reoccurs following each trigger. In fact, this technique can be used to interrogate oscillations that are not periodic or precisely repeatable.

Of the many natural oscillations known to affect Hall thruster performance, the dominant oscillation is typically the breathing mode<sup>4</sup>. This mode is characterized by oscillating depletion and replenishment of neutrals near the thruster exit at a frequency of about 10-25 kHz, and can be described by a predator-prey model for fluctuations<sup>5</sup>. Until relatively recently, Hall thruster studies have usually focused on plasma properties averaged in time. Such research is reaching maturity while many questions remain about the time-dependent behavior of Hall thruster plasma, such as how the Hall thruster breathing mode affects operation and erosion.

LIF studies using a CW laser often use a lock-in amplifier to recover the LIF signal from the strong background light emitted by the discharge. The raw signal-to-noise ratio (SNR) of this signal is typically so poor that the lock-in amplifier must be set to an integration time constant of at least 100 ms, destroying time resolution.

Significant progress has been made in recent years toward measuring TRLIF signals in similar plasma sources. Most examples employ some form of averaging in the time domain triggered off of the phase of an oscillation of the plasma source. For example, one TRLIF approach for a pulsed plasma source uses a lock-in amplifier with a short integration time constant and an oscilloscope set to average over many time-series triggered at the beginning of a pulse, improving SNR while preserving time resolution<sup>6-8</sup>.

One TRLIF approach more closely related to our goal of interrogating the Hall thruster breathing mode uses a discriminator and multichannel scaler to directly average time-series of photon counts collected over many oscillation periods. This system averages out noise by using a low-frequency laser modulation (20 Hz), adding counts collected when the laser is on (signal plus noise) and subtracting counts collected when the laser is off (noise only)<sup>9,10</sup>. When applied to study Hall thruster breathing mode oscillations, the need for repeatable triggering of each time-series was overcome by periodically cutting off the thruster discharge current for a short time and triggering each time-series based on that cutoff. The plasma at reignition resulted in quasi-periodic oscillations that behaved much like natural breathing mode oscillations, but the velocity distribution was found to be changed by the perturbation in discharge current<sup>11</sup>.

More recently, MacDonald, Cappelli, and Hargus implemented a TRLIF system that uses a sample-and-hold circuit to hold the signal level at a given phase of the oscillation and send that signal into a lock-in amplifier to recover the signal from the noise<sup>12</sup>. Since the signal into the lock-in amplifier is held at a certain phase of the oscillation, time-resolved signal recovery is made possible using a low-frequency laser modulation of 11 Hz and a typical commercial lock-in amplifier.

Most recently, we have adapted the transfer function averaging technique developed by Lobbia *et al.* for work on high-speed Langmuir probes<sup>1-3</sup> to TRLIF measurements. The laser modulation frequency (~MHz) is above the time scale of interest (~10 kHz), allowing band-pass filtering and phase-sensitive detection (PSD) with a short time constant (~μs) to raise SNR and demodulate the signal while preserving time-resolved information. Further averaging is necessary to recover a reasonable SNR due to the short time constant, hence the need for transfer function averaging. In some circumstances, this frequency-domain TRLIF technique offers advantages over the aforementioned time-domain TRLIF methods.

The main advantage of frequency-domain TRLIF is that finding or forcing some form of trigger is unnecessary, as the initial phase of each time-series used in averaging is immaterial. This feature is advantageous in the case of the Hall thruster breathing mode, where amplitude and period of individual oscillations vary due to the inherently chaotic nature of the discharge current and its complicated Fourier spectrum. This system permits measurements on actual thruster operating conditions without resorting to any kind of perturbation to create a trigger for averaging, which was found necessary for triggering in previous studies in a Hall thruster<sup>10</sup>.

In addition, for systems that have a relatively complicated Fourier spectrum with oscillations that vary in amplitude and period (such as the Hall thruster breathing mode), another advantage is that the transfer function can model the LIF signal without an unphysical decay in the oscillation amplitude. Such decay can be an artifact of performing triggered ensemble averaging when the period of oscillation changes because the many traces in the ensemble average tend to become out of phase at longer times after the trigger.

An advantage shared by techniques using fast laser modulation, filtering, and phase-sensitive detection is that the total acquisition time is reduced since a large part of the noise spectrum can be rejected before averaging over many oscillation cycles. This ultimately enables the system to either interrogate more spatial points or make more closely-resolved velocity measurements over the same campaign time.

## II. Experimental Instrument

The experimental setup is summarized in Figure 1. We pump the  $5d[4]_{7/2} \rightarrow 6p[3]_{5/2}^{\circ}$  transition of singly-charged xenon (Xe II) at 834.953 nm (vacuum). The metastable Xe II ion velocity distribution function (VDF) is measured by collecting fluorescence at 541.9 nm. We use a CW tunable diode laser (Toptica TA Pro) that has a typical output power of about 200 mW and a 20-50 GHz mode hop free range. The beam is sampled and the sample beams are sent to various diagnostics: (1) a Burleigh SA-91 etalon assembly with 2-GHz free spectral range to ensure single-mode laser operation (there are typically several resonance peaks inside the frequency ranged scanned for a VDF); (2) a HighFinesse WS/7 wavemeter with an accuracy of 60 MHz; (3) a mechanical chopper and opto-galvanic cell (Hamamatsu L2783-42 XeNe-Mo galvatron) to provide a stationary wavelength reference; and (4) a Thorlabs PDA36A photodiode to monitor laser power during the experiment. A commercial lock-in amplifier is used to recover the signal from the opto-galvanic effect in the opto-galvanic cell to measure the pumped line with zero bulk ion velocity. The main laser beam is modulated by a NEOS 23080-1 acousto-optic modulator (AOM) that permits laser modulation frequencies up to about 5 MHz without significant distortion of the modulation waveform. The modulation frequency ( $f_{mod}$ ) for the data shown is 1 MHz.

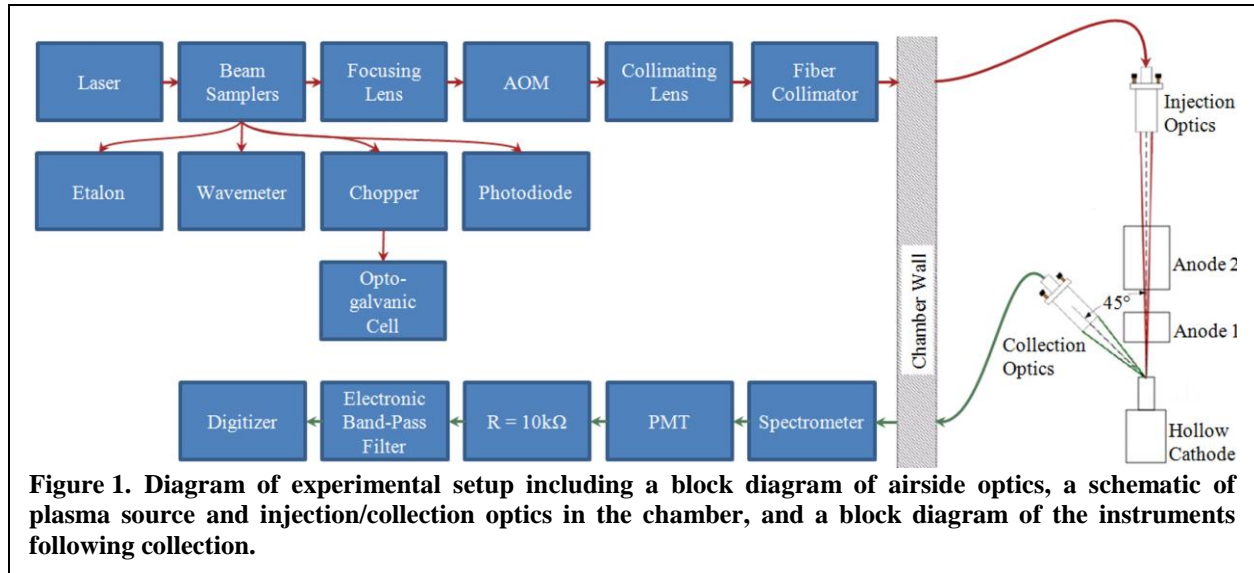


**Figure 1. Diagram of experimental setup including a block diagram of airsides optics, a schematic of plasma source and injection/collection optics in the chamber, and a block diagram of the instruments following collection.**

A pair of focusing and collimating lenses provide a reasonable balance between diffraction efficiency ( $\sim 70\%$ ) and rise time (32 ns) for the AOM. The beam is coupled to a 50- $\mu\text{m}$  optical fiber with a numerical aperture of 0.22 and delivered into the chamber by an optical fiber feed through. The beam is injected axially into the cathode orifice and focused down to a beam waist of approximately 1 mm in diameter at the interrogation point. The interrogation point location, at the edge of the keeper plate concentric with the hollow cathode orifice, was chosen to maximize SNR. A 75-mm-diameter lens with 85-mm focal length images light collected from the interrogation point onto a 1-mm optical fiber with a unity magnification. The interrogation volume, defined by the intersection of laser injection and light collection, is approximately cylindrical with a diameter of 1 mm and a length of 1 mm.

Collected light in the fiber is fed out of the chamber and into a SPEX-500M spectrometer, set to pass wavelengths near the 541.9 nm LIF transition with a bandwidth of about 1 nm. Light is then converted to an electrical signal by a Hamamatsu R928 photomultiplier (PMT), which is terminated by a 10-k $\Omega$  resistor for fast response. Fourth order Butterworth band-pass filtering and amplification of the signal is provided by a Krohn-Hite 3945 programmable electronic filter, with cutoff frequencies at 0.9 and 1.1 MHz.

Finally, the output from the filter is recorded by an Alazartech 9462 digitizer set to stream continuously to disk for 60 s per wavelength; input and output amplification on the filter are set to fill the digitizer input range as well as possible. The digitizer has 16-bit resolution, a maximum sample speed of 180 MHz, and a selection of input full scale ranges from  $\pm 200$  mV to  $\pm 4$  V. The discharge current, measured by a Tektronix TCP 312 current probe, is simultaneously sampled by the second channel of the 9462 digitizer for use in post-processing.

Since the data rate at the full 180 MHz sample speed is nearly 1 GB/s, we solve the considerable data transfer and storage requirements by streaming directly to a RAID of 10 hard drives with a net capacity of 16 TB. After optimizing system parameters, we found good results with a 20-MHz sample rate; thus, each single-wavelength, 60-

s measurement results in a 4.5 GB data set. We custom built a PC with dual hexacore Intel Xeon CPUs and 72 GB of RAM to analyze multiple data sets in parallel and to house the digitizer and RAID for data acquisition.

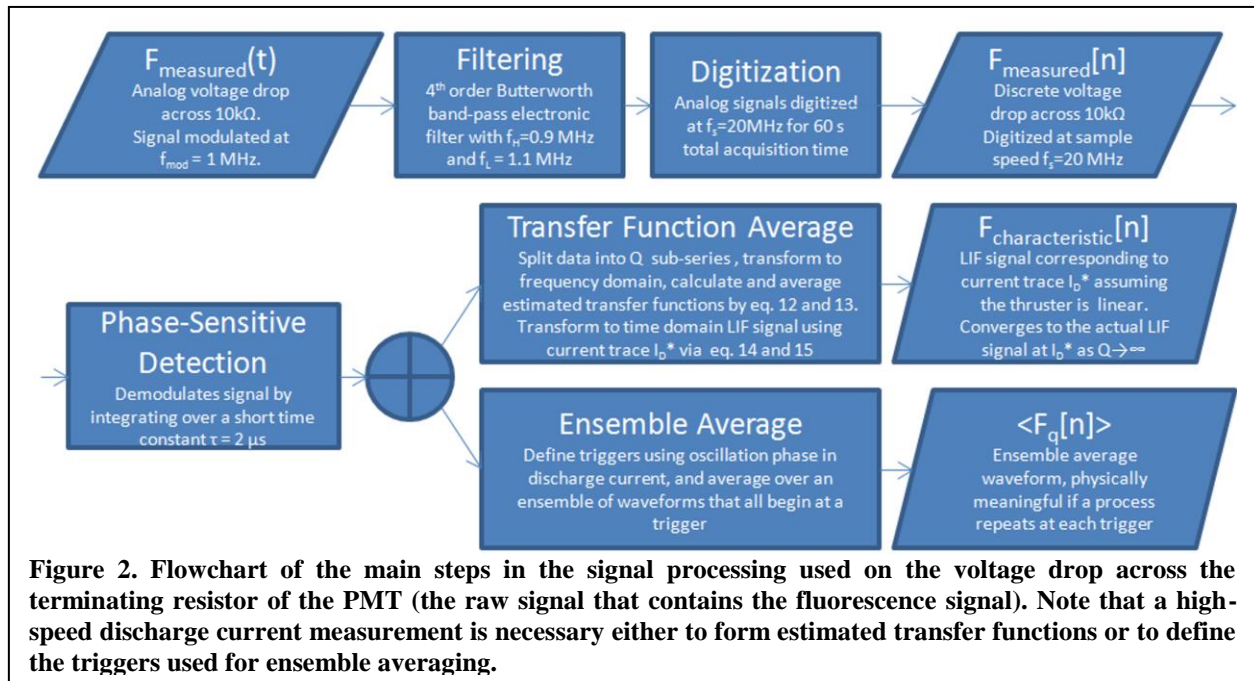
The plasma source is an orificed hollow cathode<sup>13,14</sup> that was originally designed as the ionization stage cathode of the NASA-173GT, a two-stage hybrid Hall/ion thruster<sup>15</sup>. It was custom made by the Busek Corporation and has a nominal discharge current up to 60 A. Though the cathode has a nominal 10-sccm flow rate, the LIF signal was not measurable at 10 sccm. We operated at 3.5 sccm, where the LIF signal was maximized, for this test. Loss of LIF signal at higher flow rates is likely due to collisional quenching of the metastable state in higher background pressure. The test was performed in "Junior," which is a 1-m-diameter by 3-m-long chamber connected to the much larger (6-m by 9-m) Large Vacuum Test Facility via a gate valve. Junior uses a turbopump as its primary pump, providing a base pressure of  $2 \times 10^{-6}$  Torr and a background pressure during cathode operation of  $4 \times 10^{-5}$  Torr.

To establish a highly controllable discharge current oscillation, the experiment used a pair of anodes powered by bipolar power amplifiers (a Kepco 100-2M and a Kepco 100-4M) in current control mode. The anodes are 7.6-cm-diameter rings made of 0.635-mm-thick stainless steel. Anode 1 is 5 cm long, positioned 10 cm from the cathode keeper plate, and supported by the 2-A supply. Anode 2 is 10 cm long, positioned 18 cm the cathode, and supported by the 4-A supply. The total discharge current is the sum of currents in both anodes. Two anodes were used with power amplifiers because a single high-speed amplifier could not supply sufficient current for a stable discharge and strong LIF signal. The same control signal was used for both current amplifiers, and the discharge current was found to be extremely stable in the range of approximately 4-6 A. A 10-kHz sine wave was used to approximate the frequency of a Hall thruster breathing mode. The heater and keeper were left on during operation to help stabilize the discharge.

One reason to use a hollow cathode for validation is to control the discharge current more easily than is possible with a Hall thruster. If the discharge current oscillates periodically, then the oscillation of plasma parameters should be periodic as well, turbulent and stochastic effects notwithstanding. That allows the easy use of triggered ensemble averaging with the discharge current as a phase reference, which we use as a key part of the argument for validation.

### III. Signal Processing

A simplified block diagram of the main steps in signal processing to recover TRLIF signal is shown in Figure 2. The idea of the new method is to use high speed laser modulation and then use band-pass filtering and phase-sensitive detection as signal conditioning to improve SNR and demodulate the signal before averaging over



estimated transfer functions. Alternatively to transfer function averaging, we also apply triggered ensemble averaging of signal waveforms directly in the time domain as part of the validation test for transfer function

averaging. The following subsections will describe the process and purpose of each of these steps in signal processing.

### A. Band-Pass Filtering

The LIF signal, modulated at the laser modulation frequency  $f_{mod}$ , is buried in noise that has a nonwhite spectral density with much greater density at frequencies lower than about 1 MHz. Figure 3 is an example of measured noise spectral density in the photomultiplier signal from a Hall thruster. The calculated Johnson noise for a 10k $\Omega$  resistor and the nominal input noise of the Krohn-Hite 3945 are also plotted to demonstrate that background emission dominates noise.

A signal conditioning band-pass filter greatly reduces noise from frequency components far from the modulation frequency, improving SNR and making the signal easier to digitize. The band-pass filter used for signal conditioning in this test, provided by the Krohn-Hite 3945, was a low-pass filter with a cutoff frequency of 1.1 MHz followed by a high-pass filter with a cutoff frequency of 0.9 MHz, both 4th order Butterworth filters. The filter passes the signal with little modification, but rejects a large portion of the noise spectrum, leading to an SNR improvement after the band-pass filter of 53 for the measured noise spectral density and about 4 for white (constant) noise spectral density. Therefore, this signal conditioning gives a large improvement when the noise spectral density is relatively low near the modulation frequency and high for some other frequency band, and improvement is relatively lower for a more uniform spectral density.

The signal is digitized immediately following the signal conditioning by the electronic filter. All signal processing following occurs digitally in post processing after the experiment.

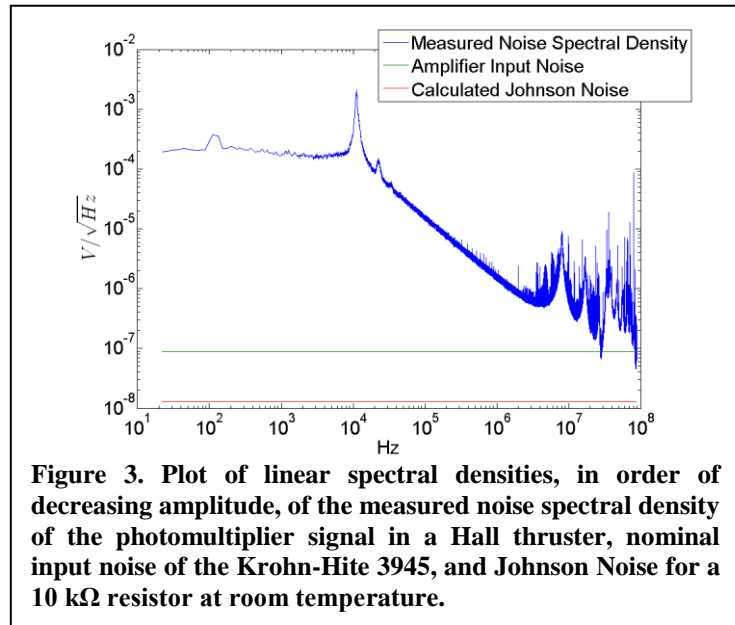


**Figure 3. Plot of linear spectral densities, in order of decreasing amplitude, of the measured noise spectral density of the photomultiplier signal in a Hall thruster, nominal input noise of the Krohn-Hite 3945, and Johnson Noise for a 10 k $\Omega$  resistor at room temperature.**

### B. Phase-Sensitive Detection

The SNR is greatly improved following band-pass filtering, but the desired LIF signal is still modulated at the laser modulation frequency and buried in noise. The desired TRLIF signal is the envelope  $m(t)$  of this modulated signal  $F(t)=m(t)\sin(\omega_{mod}t)$ . The purpose of phase-sensitive detection (PSD) is to demodulate the signal so that averaging in the next analysis step can recover the envelope with high SNR. Phase-sensitive detection is the algorithm used by lock-in amplifiers to recover a small signal at a known reference frequency from a strong noise floor or background signal. Using a lock-in amplifier integrating over a large time constant is the conventional method to measure the time-averaged LIF signal.

Briefly, phase-sensitive detection multiplies the input signal by a reference signal at a known reference frequency (a sine wave reference is used in this work) and then applies a low-pass filter, effectively integrating over a time constant that depends on the cutoff frequency of the low-pass filter as  $\tau=1/2\pi f_c$ , where  $f_c$  is the cutoff frequency. To understand how this process demodulates a signal and rejects noise, consider the case where the input signal is itself a sine wave at frequency  $f$ . Then the product of the input and reference signals will have components at frequencies  $|f+f_{ref}|$  and  $|f-f_{ref}|$  by a trigonometric identity. If we consider the input signal as composed of many frequencies in a Fourier spectrum, then the product will only have a DC component proportional to the sine wave amplitude when  $f=f_{ref}$ . The low-pass filter acts to pass that desired DC signal while removing contributions from noise at other frequencies (which will never have a DC or low frequency component after mixing with the reference signal except when noise is near the reference frequency). In general, the detector must integrate over many reference periods to recover the signal.

We can think of a phase-sensitive detector as having a "transmission window" that is defined by the cutoff frequency of the low pass filter and will pass noise components that satisfy  $|f-f_{ref}| < f_c$ . The trade off is that although a lower filter cutoff frequency rejects more noise components while passing the signal (thereby raising SNR), it

raises the integration time constant (thereby destroying time-resolved information). The settling time for the signal output with a first order filter is about 99% signal after  $5\tau$  time. Thus, time resolution will be limited to at best a few time constants. These considerations and more are discussed in detail in reference 16, which is a classic monograph on PSD and lock-in amplifiers.

In this situation, instead of a simple sine wave, we have an envelope that is modulated at the reference frequency. The signal will be demodulated and the envelope passed as a low-pass filtered version of the envelope. Hence the envelope will be faithfully passed if there are no significant frequency components above the low-pass cutoff. Conversely, if all significant AC components are above the cutoff then only the DC component will be passed and the output will be proportional to the time-average of the envelope waveform. This fact is implicitly used to justify comparing the time-average TRLIF profiles with the average LIF profile from a lock-in amplifier set to a long time constant, since this fact implies the two measurements are equivalent.

The primary point to note for our purposes is that in order to preserve time-resolved information while using phase-sensitive detection, ideally we would like to satisfy the following double inequality:

$$T_{ref} \ll \tau \ll T, \quad (1)$$

where  $T_{ref} = 2\pi/\omega_{ref}$  is the period of the reference sine wave at a frequency of  $\omega_{ref}$ ,  $\tau$  is the integration time constant, and  $T$  is the time scale of interest over which we would like to resolve change in the signal. The left hand inequality follows from the requirement of phase-sensitive detection to average over many reference periods to recover the signal, while the right hand inequality is a statement that time-resolved information is destroyed when we integrate over a time constant. The signal may not be reliably recovered if the left side is insufficiently satisfied, although in practice signal recovery is still possible even if the time constant is only a small factor larger than the reference period since averaging is effectively done over a few time constants. If the right side is poorly satisfied then features will be smoothed because PSD is averaging data over a relatively long time.

Now, we have chosen a discharge current oscillation frequency of 10 kHz for the hollow cathode to simulate the frequency of Hall thruster breathing and spoke modes, the measurement of which is the goal for this system. Such a measurement requires a resolved time scale of order  $T = 10^{-5}$  s, since we require at least a few points inside each breathing mode period. The fastest reference frequency possible would be ideal since the noise spectrum is approximately pink, but our AOM can reach almost 10 MHz (order  $T_{ref} = 10^{-7}$  s). This places a fairly strict order-of-magnitude requirement on the integration time constant of  $\tau = 10^{-6}$  s. Because we must integrate over such short time scales and the SNR improvement factor is proportional to the square root of the time constant, then this gives only a modest improvement to SNR and further averaging is necessary. We calculate that the SNR improvement is about 4 in this case for  $\tau = 2 \times 10^{-6}$  s. Hence the use of phase-sensitive detection acts to demodulate the signal but it will not provide a major improvement to SNR when used with such short time constants, and we require further averaging over many oscillation cycles.

The final step in analysis is an ensemble average over either the PMT signal after filtering and phase-sensitive detection ("triggered ensemble averaging"), or over estimated transfer functions derived from that signal and the discharge current signal ("transfer function averaging"). We begin by considering the case of transfer function averaging.

### C. Fourier Analysis and Transfer Function Averaging

The step that produces the largest improvement in SNR is the transfer function averaging technique first used with high-speed Langmuir probes<sup>1</sup>. Using the terminology of systems and signals from the field of signal processing, the idea is to assume the thruster acts essentially as a linear system in the sense that the discharge current is the system input signal that leads to output signals of plasma properties in the plume (such as density or ion velocity at a point). Some plasma behavior is stochastic and therefore necessarily nonlinear, but linear characteristic features can exist and dominate behavior. The assumption of linearity was ultimately justified by Lobbia by noting that the synthesized signals from transfer functions matched all the key features of the original density signals for the same input current signal<sup>2</sup>.

Consider discrete signal vectors  $I_D[n]$  and  $F[n]$ , which are ideal discharge current and fluorescence signals measured in the absence of noise. This ideal fluorescence signal corresponds to the density of a population of ions in the interrogation zone having a velocity corresponding to the Doppler-shifted laser wavelength. Both signals are discretely sampled  $N$  times, and  $n$  is the index of a particular sample, so  $0 \leq n \leq N-1$ . If the system is linear then there is a transfer function  $H[k]$  relating any two simultaneous input and output spectra:

$$\tilde{F}[k] = H[k]\tilde{I}_D[k]. \quad (2)$$

The index for the Fourier space is  $k$ , which has the same range as  $n$ . It is our convention in this paper to use a tilde to denote the discrete Fourier transform, i.e. any pair of signals written with/without a tilde are related by the discrete Fourier transform (DFT):

$$\tilde{A}[k] = \sum_{n=0}^{N-1} A[n] \exp(-2\pi i k n / N). \quad (3)$$

Now, consider the measured signals, which we model to be composed of the ideal signals plus an additive noise sequence of random variables with some probability distribution with zero mean (since this signal is following filtering and phase-sensitive detection). The fluorescence signal is buried in noise, while the discharge current signal from the current probe is very precise:

$$\begin{aligned} F_{measured}[n] &= F[n] + N_f[n] \\ I_{D,measured}[n] &= I_D[n] + N_I[n] \approx I_D[n] \end{aligned} \quad (4)$$

Then we can estimate the transfer function by simultaneously measuring the input and output signals and dividing their spectra elementwise:

$$\begin{aligned} H_{estimated}[k] &= \frac{\tilde{F}_{measured}[k]}{\tilde{I}_{D,measured}[k]} \approx \frac{\tilde{F}[k] + \tilde{N}_f[k]}{\tilde{I}_D[k]} = H[k] + N_H[k] \\ N_H[k] &= \frac{\tilde{N}_f[k]}{\tilde{I}_D[k]} \end{aligned} \quad (5)$$

The estimated transfer function is also buried in noise since the fluorescence signal is. During the experiment, we simultaneously digitize a series of  $N$  points of discharge current  $I_{D,measured}[n]$  and photomultiplier signal  $F_{measured}[n]$  for a total duration of about 60 s at a sampling frequency  $fs = 20$  MHz with the laser set to a constant wavelength. The long series (~60 s) of  $N$  points is split into  $Q$  sub-series of  $N/Q$  points each. We then find a transfer function estimate for each sub-series and average to obtain an average estimated transfer function:

$$\langle H[k] \rangle = \frac{1}{Q} \sum_{q=1}^Q H_{estimated,q}[k] = \frac{1}{Q} \sum_{q=1}^Q H[k] + N_{H,q}[k] = H[k] + \frac{1}{Q} \sum_{q=1}^Q N_{H,q}[k] \quad (6)$$

Note that  $N_{H,q}[k]$  is a complex random variable sequence with zero mean since  $\tilde{N}_f[k]$  is and they are related by a linear transformation with no additive constant. In turn,  $\tilde{N}_f[k]$  has zero mean since  $N_f[n]$  does and they are related by the discrete Fourier transform, which is in this case a sum of linearly transformed random variables where the linear transform never has an additive constant. Then by well known properties of sums and linear transformations of random variables, the average in the final term in equation (6) is itself a sequence of complex random variables with zero mean and variance reduced by a factor of  $Q$  relative to the average variance of  $N_{H,q}[k]$ . This an example of the classic result that in general averaging  $Q$  measurements improves SNR by a factor of  $\sqrt{Q}$ . Therefore we can say the average estimated transfer function approaches the exact transfer function in the limit that  $Q$  approaches infinity.

The average transfer function is then characteristic of the linear behavior of the thruster. Approximate values of  $Q = 10$  or  $Q = 100$  were used to average out turbulence and noise in Lobbia's work. In this work, transfer function averaging is the primary form of averaging to improve SNR from the PMT signal, hence we use values of approximately  $Q = 100,000$ .

We are now in a position to synthesize the system's characteristic response  $F_{characteristic}[n]$  (the characteristic time-resolved LIF signal at the interrogation point corresponding to the laser wavelength) to an arbitrary input signal  $I_D^*[n]$ , the discharge current signal for which we want to calculate the characteristic response. This can be any discharge current signal series of length  $N/Q$ . Since they are all similar in terms of spectral content, we typically choose the last one used in post-processing. Given an average transfer function, the system characteristic response to the input is:

$$\tilde{F}_{characteristic}[k] = \tilde{I}_D^*[k] \langle H[k] \rangle, \quad (7)$$

and we transform back to the time domain by an inverse DFT on the characteristic spectrum:

$$F_{characteristic}[n] = \frac{Q}{N} \sum_{k=0}^{N-1} \tilde{F}_{characteristic}[k] \exp(2\pi i k n Q / N). \quad (8)$$

The result of each transfer function is the VDF amplitude as a function of time at a velocity corresponding to the Doppler-shifted ion absorption wavelength. The same procedure is repeated for all wavelengths desired to build up the ion VDF profile. At least about 10 wavelengths are necessary to resolve the VDF reasonably well in both velocity space and time.

It is important to note that the same input discharge current signal,  $I_D^*[n]$ , is used to synthesize data for all wavelengths. This is so that the synthesized response at each wavelength corresponds to a common input signal, ensuring coherent responses at all points over a long time scale. This is an important feature of averaging in the frequency domain. The raw data series at each wavelength are all incoherent with each other since they are taken with some arbitrary time delay between them. Using the transfer function averaging technique requires no triggering, yet signals synthesized from the same input are all coherent and can be meaningfully plotted together in a visualization of the VDF.

In this paper we present results only at a single spatial location for the purpose of validating the new technique and system, but the same idea applies to creating a visualization of a full thruster plume. We would capture enough data to form average transfer functions for all wavelengths and spatial locations of interest, and then use the same input discharge current signal to synthesize the characteristic response for all of them.

Since other time-correlated methods use forms of triggered ensemble averaging over many periods of oscillation, it is of interest to determine how the characteristic LIF signal resulting from the transfer function average relates to the ensemble average result. First, consider an arbitrary discharge current measurement  $I_D^*[n]$  of length  $N/Q$ . If the assumption of linearity holds, then the average transfer function converges to the exact system transfer function as described above. Then by equation (2) the characteristic LIF signal spectrum converges to the exact spectrum of the LIF signal corresponding to the same time as  $I_D^*[n]$ , and therefore  $F_{characteristic}[n]$  converges to the exact time domain fluorescence signal corresponding to that time. Therefore, the output of the linear model converges to the ideal LIF signal at the time of the input discharge current trace, if the assumption of a linear system is justified.

This technique models the LIF signal as output related by a linear system to an input discharge current signal. It requires averaging over a sufficient number of input and output signals so that the estimated transfer function sufficiently converges, but there is no explicit assumption that a repeatable process is occurring; only that the system is linear and transfer function itself is constant. This is in contrast to techniques using an ensemble average triggering at some feature that is assumed to be the beginning of some repeatable process.

#### D. Triggered Ensemble Average

At this stage (following phase-sensitive detection, see Figure 2), the signal is demodulated and following its original envelope, which corresponds to the population of ions in the interrogation volume with the velocity associated with the laser wavelength. We again model this measured signal as composed of the sum of the ideal LIF signal and some noise signal, which is assumed to be a sequence of independent random variables distributed by some probability distribution function with zero mean and some variance  $\sigma_F^2$ . The noise will have zero mean at this stage because noise signals near the modulation frequency that are passed by PSD will be incoherent with the reference signal and therefore have randomized sign.

As an alternative to transfer function averaging, we use triggered ensemble averaging as part of the validation argument. An ensemble average takes an ensemble of measurement traces and averages them together elementwise (i.e. all of the same time points from each waveform are averaged together). The main implicit assumption of triggered ensemble averaging is that there is a repeatable process that reoccurs at each trigger, thus we can consider the ideal LIF signal at the  $n^{\text{th}}$  time point after the  $q^{\text{th}}$  trigger to be composed of the average signal and some fluctuation that may change due to small differences in the processes that occur over each trigger event. If the assumption that the same process reoccurs were exactly true, then the fluctuation would be zero for all traces; but in general this is not true. The measured signal is:

$$F_q[n] = F_{av}[n] + F_{fluc,q}[n] + N_{F,q}[n], \quad (9)$$

where  $F_{av}[n]$  is the average fluorescence signal,  $F_{fluc,q}[n]$  is some fluctuation in LIF signal during the  $q^{\text{th}}$  trigger, and  $N_{f,q}[n]$  is the noise sequence.

The idea of an ensemble average scheme is to find triggers in the phase of the discharge current that indicate the phase of the repeatable process so that we can average the LIF signal traces at the same phase to recover the average signal waveform:



$$\begin{aligned} \langle F_q[n] \rangle &= \frac{1}{Q} \sum_{q=1}^Q F_q[n] = \frac{1}{Q} \sum_{q=1}^Q F_{av}[n] + F_{fluc,q}[n] + N_{F,q}[n] \approx F_{av}[n] + \frac{1}{Q} \sum_{q=1}^Q N_{F,q}[n], \\ &\approx F_{av}[n] + R(\mu = 0, \sigma^2 = \sigma_F^2 / Q) \end{aligned}, \quad (10)$$

where  $F_{fluc,q}[n]$  averages to zero in the limit since by definition the average LIF signal is  $F_{av}[n]$ . Also, since  $N_{f,q}[n]$  is a sequence of random variables, then the average of  $Q$  such variables will be a random variable sequence with the same mean ( $\mu=0$ ) and a variance that is reduced by a factor of  $Q$ . Note that this average waveform is only physically meaningful in the limit that the fluctuations from the average waveform that occur after each trigger are small.

## IV. Results

We have designed a series of tests to validate the system using a hollow cathode with an oscillating discharge current as a test bed. When taken together, these tests provide strong evidence for the general validity of the technique and accuracy of the results for the system that we have implemented. Results under conditions not explicitly tested here (such as the more complicated plasma dynamics of the Hall thruster) may be considered reasonably reliable based on the foundation laid in these tests, as well as by careful consideration of how TRLIF measurements agree with other high-speed measurements (e.g. high-speed Langmuir probe<sup>3</sup> and high-speed framing camera<sup>17,18</sup>), as well as with theory and simulation.

### A. Output TRLIF Signal Under Incorrect Conditions

Note that analysis yields a significant TRLIF signal only when applied at the correct reference frequency to a data set captured when the laser interacts with the plasma. If analysis is applied at an incorrect reference frequency or if the laser intensity is zero, then the "signal" returned by this analysis technique is at least an order of magnitude lower than a significant TRLIF signal and its waveform resembles white noise.

In other words, the technique measures signal if and only if the conditions are correct for a signal to be measured. This is clearly a necessary feature of any accurate measurement, but it is important to note this criterion here because we apply a complicated and unusual analysis technique that could potentially be susceptible to some form of artifact. For example, the discharge current signal is used in transfer function averaging and TRLIF signals tend to have similar a Fourier spectrum as the discharge current, hence it is plausible that there might be some artifact that could cause the output TRLIF signal to have similar frequency components as the discharge current even if there is no actual LIF signal. The fact that the system measures a signal only under the proper conditions implies that there is no such artifact in analysis that creates a false LIF signal in the output and that the output LIF signal does indeed come from LIF.

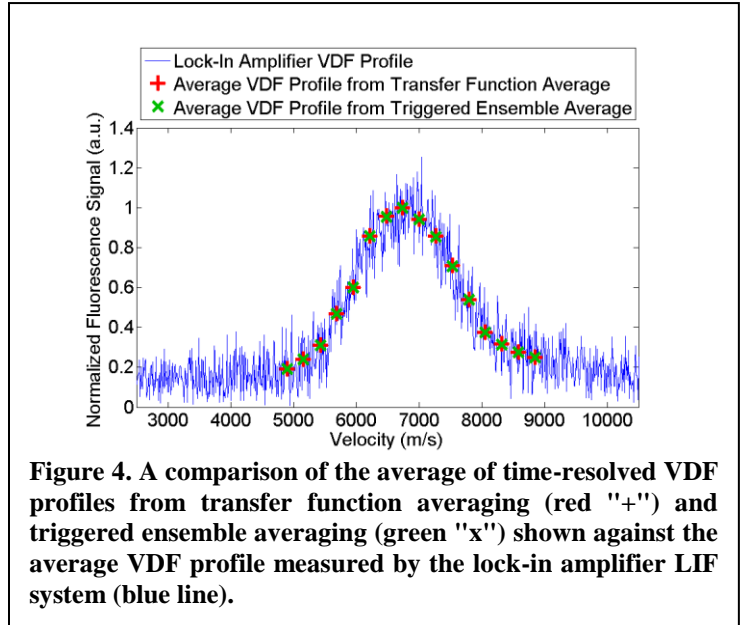


**Figure 4. A comparison of the average of time-resolved VDF profiles from transfer function averaging (red "+") and triggered ensemble averaging (green "x") shown against the average VDF profile measured by the lock-in amplifier LIF system (blue line).**

### B. Comparison of Time-Averaged TRLIF with Conventional LIF

We begin validating the accuracy of the results by comparing a time average of the TRLIF profile with the average LIF profile measured with a commercial lock-in amplifier; i.e. conventional time-averaged LIF data. An example of this comparison for the cathode experiment is shown in Figure 4. Both profiles have been normalized to unity peak magnitude, with the (noisier) lock-in amplifier signal normalized by the maximum of its smoothed profile. The profiles agree within the error of the lock-in amplifier measurement, which is roughly apparent because

there are many closely spaced points. This confirms that the average LIF profile measured with the new system agrees with the conventional measurement of a lock-in amplifier.

### C. Comparison of Transfer Function Averaging vs. Triggered Ensemble Averaging

In principle, the time-resolved features of the VDF profile could be badly distorted even if the average values are accurate, so we must go beyond the average signal comparison and validate time-resolved features as well. The transfer function averaging technique in particular is uncommon and probably is the part of analysis that is most open to doubt. We verify that the transfer function averaging technique is not introducing systematic error by applying another independent analysis technique to the same data to ensure to ensure the results agree. The independent technique used is the triggered ensemble averaging technique discussed in the signal processing section above.

Since the same data set is used in both analyses, the laser modulation and PMT signal filtering are the same for each. In order to demodulate the signal, both analyses use phase-sensitive detection with the same time constant of  $2 \mu\text{s}$ . The two analyses differ in that one analysis used the transfer function averaging technique in the frequency domain, and the other applied triggered ensemble averaging in the time domain (see Figure 2). Both were implemented in software to be done in post-processing. For ensemble averaging, the beginning of each time-series is triggered in time when the sinusoidal discharge current oscillation reaches zero phase; i.e. when it crosses through its average value with a positive slope. As discussed in the Signal Processing section, a time-series is formed from data taken for a predetermined length of time after each trigger, and all of the time-series are averaged together in an ensemble average. Note that this technique using PSD and ensemble averaging is equivalent to the technique employing a lock-in amplifier and triggered averaging by an oscilloscope<sup>6-8</sup>. The difference is that in this case the experiment is more flexible but has much more overhead because the analysis is done in software in post processing, whereas in that case PSD and averaging were done in real time with a commercial lock-in amplifier and oscilloscope.

The VDF profile is built up from TRLIF data at many wavelengths using both averaging techniques so that the complete VDF profiles can be compared to determine whether there is any distortion of the VDF profile by the transfer function technique. Heat maps of the two results and their residual (the difference between the two) as a function of time are shown in Figure 5. The two signals are close at all times and the residual appears to be due to only random noise and not any kind of systematic error. The mean of the absolute value of the residuals is 0.07, or 7% of the peak value.

A plot of two "snapshots" of the VDF profile in time is shown for both averaging techniques in Figure 6 to more clearly show the shape and behavior of the VDF profile. The VDF profile is somewhat coarse since there are only 16 points in velocity, but it is

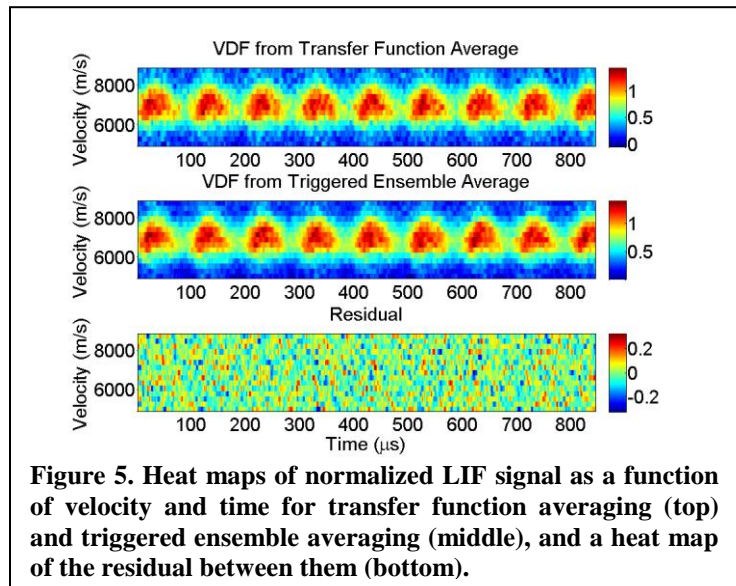


**Figure 5. Heat maps of normalized LIF signal as a function of velocity and time for transfer function averaging (top) and triggered ensemble averaging (middle), and a heat map of the residual between them (bottom).**

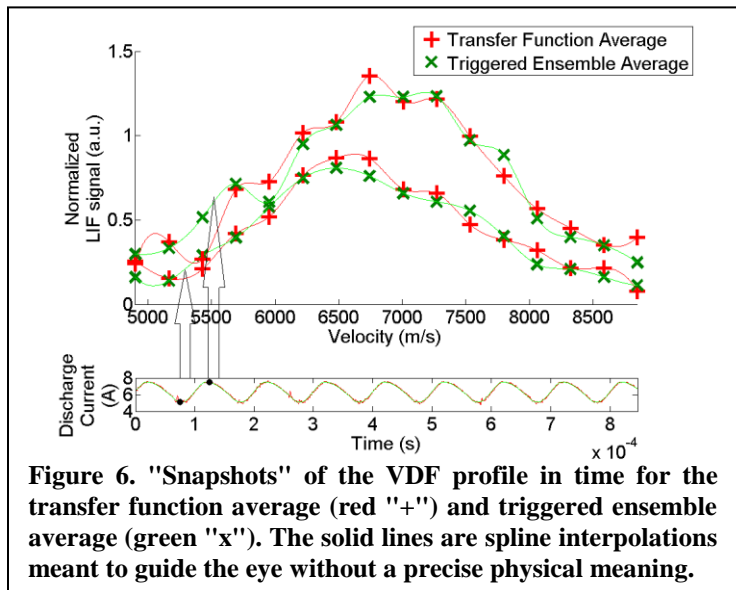


**Figure 6. "Snapshots" of the VDF profile in time for the transfer function average (red "+") and triggered ensemble average (green "x"). The solid lines are spline interpolations meant to guide the eye without a precise physical meaning.**

clear nonetheless that both techniques capture the same general features in the profile at all times, such as the mean and spread of the profile, including the slight acceleration of the mean velocity with increasing discharge current.

## V. Conclusion

A novel technique to measure TRLIF signals was developed and a system implementing the technique was tested using a hollow cathode for a test bed. The laser is modulated on the order of 1 MHz and the data are sampled at 20 MHz to use filtering, phase-sensitive detection, and Fourier analysis to recover the time-resolved signal. Fluctuations in the ion VDF caused by an oscillating discharge current at 10 kHz were observed. Measurements were validated by comparison to average VDF measurements from a typical lock-in amplifier system, as well as by comparison to time-resolved results from triggered ensemble averaging. The results from all three independent techniques agree very well.

Further experiments are planned to interrogate oscillations in Hall thruster plumes. Interesting time-dependent behavior is likely to be observed that may provide insight into Hall thruster operation and be useful for validating models. There is already reported evidence of oscillations in ion velocity distribution and electric field in the plume of a Hall thruster<sup>9-11</sup>. There have also been measurements of a bimodal average ion VDF at some locations in the plume of a 6 kW Hall thruster<sup>19</sup>. The bimodal average distribution may be a manifestation of a strongly oscillating ion distribution due to movement of the acceleration and ionization zones during the breathing mode oscillations.

The new technique described here has a niche where there is strong background signal with nonwhite spectral density and where oscillations are not repeatable enough to enable triggered averaging in the time domain. The form of noise spectral density observed in the PMT signal allows the use of high-speed laser modulation, filtering, and phase-sensitive detection to reject a large portion of the noise, improving SNR before averaging over many oscillations and therefore reducing the acquisition time. More importantly, the technique of averaging over transfer functions in the frequency domain dispenses with the need for triggering averaging at a particular phase of oscillation. We have argued that this is advantageous for oscillations that are not periodically repeatable because: (1) there is no need to perturb the operating condition to create triggers; and (2) there will be no unphysical artifacts such as a decay in the oscillation amplitude that can be observed in the average waveform when oscillations in the ensemble average drift out of phase from each other after the initial trigger. Hall thruster breathing oscillations are known to be highly non-periodic, and therefore this technique may be advantageous to use in future work interrogating Hall thrusters and other plasma sources exhibiting similar non-repeatable oscillations.

## Acknowledgements

This work was supported by AFOSR and AFRL through the MACEEP center of excellence grant number FA9550-09-1-0695. We would like to thank Drs. Mitat Birkan and Daniel Brown, the MACEEP program managers from AFOSR and AFRL, respectively.

## References

- <sup>1</sup>Lobbia, R.B. and Gallimore, A.D., "A Method of Measuring Transient Plume Properties," *44th AIAA/ASME/SAE/ASEE Joint Propulsion Conference*, Hartford, CT, 2008
- <sup>2</sup>Lobbia, R. B. and Gallimore, A. D., "Fusing Spatially and Temporally Separated Single-point Turbulent Plasma Flow Measurements into Two-dimensional Time-Resolved Visualizations," *12th International Conference on Information Fusion*, Seattle, WA, 2009.
- <sup>3</sup>Lobbia, R. B. and Gallimore, A. D., "High-speed dual Langmuir probe," *Rev. Sci. Instrum.*, vol. 81, no. 073503, 2010.
- <sup>4</sup>Choueiri, E., "Plasma oscillations in Hall thrusters," *Physics of Plasmas*, vol. 8, no. 4, pp. 1411-1426, 2001.
- <sup>5</sup>Fife, J., Martinez-Sanchez, M., and Szabo, J., "A Numerical Study of Low-Frequency Discharge Oscillations in Hall Thrusters," *American Institute of Aeronautics and Astronautics, AIAA-97-3052*, Washington, DC, 1997.
- <sup>6</sup>Scime, E., Biloiu, C., Compton, C., Doss, F., Venture, D., Heard, J., Choueiri, E., and Spektor, R., "Laser induced fluorescence in a pulsed argon plasma," *Rev. Sci. Instrum.*, vol. 76, no. 026107, 2005.
- <sup>7</sup>Biloiu, C., Sun, X., Choueiri, E., Doss, F., Scime, E., Heard, J., Spektor, R., and Ventura, D., "Evolution of the parallel and perpendicular ion velocity distribution functions in pulsed helicon plasma sources obtained by time resolved laser induced fluorescence," *Plasma Sources Sci. Technol.*, vol. 14, pp. 766-776, 2005.
- <sup>8</sup>Biloiu, I.A., Sun X., and Scime, E., "High time resolution laser induced fluorescence in pulsed argon plasma," *Rev. Sci. Instrum.*, vol. 77, p. 10F301, 2006.

<sup>9</sup>Mazouffre, S., Gawron, D., and Sadeghi, N., "A time-resolved laser induced fluorescence study on the ion velocity distribution function in a Hall thruster after a fast current disruption," *Phys. Plasmas*, vol. 16, p. 043504, 2009.

<sup>10</sup>Mazouffre, S. and Bourgeois, G., "Spatio-Temporal characteristics of ion velocity in a Hall thruster discharge," *Plasma Sources Sci. Technol*, vol. 19, no. 065018, p. 9pp, 2010.

<sup>11</sup>Bourgeois G. and Mazouffre, S. , "Examination of the temporal characteristics of the electric field in a Hall Effect thruster using a photon-counting technique," in *31st International Electric Propulsion Conference*, Ann Arbor, MI, 2009.

<sup>12</sup>MacDonald, N. A., Cappelli, M. A., and Hargus, W. A. , "Time-synchronized continuous wave laser-induced fluorescence on an oscillatory xenon discharge," *Rev. Sci. Instrum.*, vol. 83, no. 113506, 2012.

<sup>13</sup>Goebel, D. M., Jameson, K. K., Watkins, R. M., Katz, I., and Mikellides, I. G., "Hollow cathode theory and experiment. I. Plasma characterization using fast miniature scanning probes," *J. Appl. Phys.*, vol. 98, p. 113302, 2005.

<sup>14</sup>Mikellides, I. G., Katz, I., Goebel, D. M., and Polk, J. E., "Hollow cathode theory and experiment. II. A two-dimensional theoretical model of the emitter region," *J. Appl. Phys.*, vol. 98, p. 113303, 2005.

<sup>15</sup>Peterson, P. Y. and Gallimore, A. D., "The Performance and Plume Characterization of a Laboratory Gridless Ion Thruster with Closed Electron Drift Acceleration," *Joint Propulsion Conference*, AIAA-2004-3936, Fort Lauderdale, Florida, July 11-14, 2004.

<sup>16</sup>Meade, M. L., *Lock-in amplifiers: principles and applications*, Peter Peregrinus Ltd., London, UK, 1983.

<sup>17</sup>McDonald, M. S. and Gallimore, A. D., "Rotating Spoke Instabilities in Hall Thrusters," *IEEE Trans. Plasma Sci*, vol. 39, no. 11, p. 2952, 2011.

<sup>18</sup>McDonald, M. S. and Gallimore, A. D., "Parametric Investigation of the Rotating Spoke Instability in Hall Thrusters," *32nd International Electric Propulsion Conference*, Wiesbaden, Germany, 2011.

<sup>19</sup>Huang, W., Drenkow, B., and Gallimore, A., "Laser-Induced Fluorescence of Singly-Charged Xenon inside a 6-kW Hall Thruster," *45th AIAA/ASME/SAE/ASEE Joint Propulsion Conference & Exhibit*, Denver, Colorado, August 2009.